

SAND99-1823J

**Differentiation of Chemical Components in a Binary Solvent Vapor Mixture
Using Carbon/Polymer Composite-Based Chemiresistors**

Sanjay V. Patel, Mark W. Jenkins, Robert C. Hughes, W. Graham Yelton, and Antonio J. Ricco¹

Sandia National Laboratories

Microsensor Research and Development Department

Albuquerque, NM 87185-1425

RECEIVED
AUG 11 1999
OSTI

Key Words: Polymer Composite; Chemiresistor; Universal Solvent Sensor Array; Vapor Sensor; Humidity; Carbon-Loaded Polymer; Pattern Recognition; polyvinyl alcohol; polyethylene vinylacetate;

¹Present address: ACLARA BioSciences, 1288 Pear Ave., Mountain View, CA 94043

DISCLAIMER

This report was prepared as an account of work sponsored by an agency of the United States Government. Neither the United States Government nor any agency thereof, nor any of their employees, make any warranty, express or implied, or assumes any legal liability or responsibility for the accuracy, completeness, or usefulness of any information, apparatus, product, or process disclosed, or represents that its use would not infringe privately owned rights. Reference herein to any specific commercial product, process, or service by trade name, trademark, manufacturer, or otherwise does not necessarily constitute or imply its endorsement, recommendation, or favoring by the United States Government or any agency thereof. The views and opinions of authors expressed herein do not necessarily state or reflect those of the United States Government or any agency thereof.

DISCLAIMER

**Portions of this document may be illegible
in electronic image products. Images are
produced from the best available original
document.**

Abstract

We demonstrate a “universal solvent sensor” constructed from a small array of carbon/polymer composite chemiresistors that respond to solvents spanning a wide range of Hildebrand solubility parameters. Conductive carbon particles provide electrical continuity in these composite films. When the polymer matrix absorbs solvent vapors, the composite film swells, the average separation between carbon particles increases, and an increase in film resistance results, as some of the conduction pathways are broken. The adverse effects of contact resistance at high solvent concentrations are reported. Solvent vapors including isooctane, ethanol, diisopropylmethylphosphonate (DIMP), and water are correctly identified (“classified”) using three chemiresistors, their composite coatings chosen to span the full range of solubility parameters. With the same three sensors, binary mixtures of solvent vapor and water vapor are correctly classified; following classification; two sensors suffice to determine the concentrations of both vapor components. Polyethylene vinylacetate and polyvinyl alcohol (PVA) are two such polymers that are used to classify binary mixtures of DIMP with water vapor; the PVA/carbon-particle-composite films are sensitive to less than 0.25% relative humidity. The Sandia-developed VERI (Visual-Empirical Region of Influence) technique is used as a method of pattern recognition to classify the solvents and mixtures and to distinguish them from water vapor. In many cases, the response of a given composite sensing film to a binary mixture deviates significantly from the sum of the responses to the isolated vapor components at the same concentrations. While these nonlinearities pose significant difficulty for (primarily) linear methods such as principal components analysis, VERI handles both linear and nonlinear data with equal ease. In the present study the maximum speciation accuracy is achieved by an array containing three or four sensor elements, with the addition of more sensors resulting in a measurable accuracy decrease.

Introduction

Sensors for organic solvent vapors are required for the detection of leaks, toxic chemicals, explosives, and solvent spills. As part of a system, these sensors need to be highly sensitive to small concentrations of vapors in ambient air, while consuming minimal power for use in portable devices. Such a sensor system must be able to quickly and reproducibly distinguish solvents from the ambient relative humidity classifying the responses as a particular solvent, relative humidity, a mixture, or unknown. The development of a single sensor to distinguish different solvents is difficult; however, sensor arrays with several sensitive devices can be used to sense a wide variety of solvents. Sophisticated pattern-recognition algorithms can aid in the analysis of signals from several sensors in an array and can be used to determine the class of analyte measured.¹⁻³ A significant amount of research has been performed to develop sensor arrays comprised of several sensitive elements.⁴

The materials used in such arrays depend upon the sensing task at hand. Catalytic films have been used for hydrogen and hydrocarbons⁵, while for solvents the most prevalent materials are polymers. Since polymer films swell upon absorption of solvents, they exhibit measurable changes in macroscopic properties. There has been significant research in developing polymer-based arrays, using three general classes of conductive, as well as non-conductive, polymers^{1-3,6}. Electronically conducting polymers comprise two classes: (1) the “organic metals”, those organic materials that are inherently conductive due to their electronic structure, typified by polyaniline, polypyrrole, polythiophene, and polyacetylene; (2) composites made from conventional, insulating organic polymer matrices, loaded with conductive particles such as carbon or silver at sufficiently high levels to form continuous conductive pathways through the matrix. Appropriately prepared films from both of these categories allow straightforward (DC) resistance measurements of film properties, without large power requirements or complex circuits. The third class of conductive film, based on ionically conductive polymeric materials—the so-called polyelectrolytes—are fabricated from a host matrix through which ions can move readily, such as polyethylene oxide (PEO), and a salt for which one or both components are mobile in the host, such as LiClO₄ in the case of PEO. These materials tend to be somewhat more resistive, and may yield confusing or irreproducible results when probed at zero frequency: the necessity for electron transfer between the electronically conductive probing electrodes and the charge-carrying ions has the unintended consequence of causing electrochemical, often permanent, change in the matrix, ions, or analytes. Thus, more complex AC measurement circuitry, which can

probe the ionic conductivity via capacitive coupling rather than direct (Faradaic) electron transfer, may be required to obtain the best results from materials.

For all three classes of conductive polymer materials, fabrication of films with reproducible behavior is often difficult. Non-conducting polymer films, typically fabricated from a single component of a conventional polymer, are often much easier to make in highly reproducible form, but are not suitable for electrical resistance measurements. Acoustic wave devices, which respond to changes in surface mass and film mechanical properties, can be used with completely insulating or any of the three types of conductive materials (if patterned so as not to short out the transducers), and are generally very sensitive; however, the high-frequency circuitry used to monitor these devices is fairly complex. The absorption of many solvents by polymers has been studied in great detail on SAW (surface acoustic wave) device arrays^{3,7,8}.

Carbon or metal-loaded-polymer-composite-based chemiresistors are an inexpensive, easily fabricated alternative for sensor arrays. The carbon or metal particles form conductive networks through the polymer films. Composite films can be made of any polymer with varied conductive particle concentration. These types of composite materials have long been used as positive-temperature-coefficient resistors in electronics, and even as chemical sensors for nearly 20 years. The composite film resistance depends strongly on the concentration of the carbon or metal and on temperature.⁹⁻¹³

If a polymer/conductive particle composite increases its volume by thermal expansion or by swelling when absorbing a chemical, the electrical resistance increases due to a breaking of some of the conductive pathways through the film. The expansion can produce large increases in resistance if the polymer volume is changed close to the percolation threshold¹²⁻¹⁴. This threshold concentration has been found to be between 20 and 40% by volume of the conductive particles. The response of these composite films to different solvents depends on the particular solvent-polymer interaction, while the conductive particles only report the degree of swelling.^{9,10} Such materials have been modeled as a network of resistors and diodes, where resistors represent the conductive network of carbon particles and diodes represent the polymer-filled dielectric gaps between the particles.¹¹

The degree of swelling of a particular polymer is related to its solubility parameter (δ) and the solubility parameter of the solvent. The solubility parameter is used to describe the free energy of mixing of non-polar, non-associating fluids, and can be extended to other solvents and to polymers, so long as the interaction process is not

exothermic. Two solvents that have identical values of δ will form ideal solutions and will have almost zero heat (enthalpy) of mixing. Such ideal solutions of two liquids follow Raoult's law: the vapor pressure of each of the solvents is proportional to the mole fraction of the solvent in the liquid phase. The amount of solvent-induced polymer swelling depends in turn on the partitioning of the solvent vapor into the polymer film.^{9,10}

The solubility parameter and the idea of partitioning of the solvent between two phases have already been studied for determining the relative responses of gas sensor arrays.^{2,8-10,15} Since it is unlikely that a specific polymer will be sensitive to only one solvent (every polymer absorbs a number of solvents having similar solubility parameters), an array of sensors is an effective means to discriminate against interfering vapors. A common and obvious source of interference is relative humidity in the ambient environment. Water vapor has been found to change the relative sensitivity of certain polymers to solvent vapors and the patterns of responses obtained from arrays containing those polymers.⁶ To build a sensor array that is capable of identifying the maximum number of analytes, the array should contain several different sensors that are as chemically varied as possible, with at least one sensor having significant sensitivity to relative humidity.

As with any such sensor array, suitable pattern recognition (PR) algorithms must be used to analyze the responses of several devices to several solvents and interfering vapors. PR methods that deal effectively with nonlinear and/or nonadditive (in the case of mixtures) sensor responses allow a much broader range of sensing film candidate materials to be considered, and they also expand the useful dynamic range to higher concentrations where responses are most often nonlinear. One such PR method, Sandia's VERI technique, is used in this paper to classify array responses from carbon/polymer composites.

Experimental Details

The polymer films used as chemiresistors were deposited on two different platforms. The first type used a pair of interdigitated electrodes on quartz substrates. These were fabricated using photolithography to pattern 50 finger pairs of gold electrodes having a chromium adhesion layer. The electrode spacing was 8 μm , the electrodes were 1.6 mm long, and the resistance was measured in a two-point-probe configuration. On the same device, a single set of widely spaced (~3 mm) electrodes, 1.8 mm long, was deposited to measure resistance of films that might have an uncharacteristically low resistance across the 8 μm spacing. The second type of platform consisted

of 6 mm long platinum electrodes with a titanium adhesion layer, on a silicon wafer that had a 100 nm thick Si₃N₄ layer for electrical insulation. The platinum electrodes were arranged in a four-point probe configuration, with two inner (10 μ m wide) and two outer (50 μ m wide) electrodes. Devices were made with an inner electrode spacing of either 100 or 50 μ m. All the electrodes, on both types of devices, were connected to large pads for external electrical contact. These data are the first reported four-terminal measurements on this type of chemiresistor, in which the bulk resistance can be separated from the contact resistance.

The carbon-loaded polymers were made by dissolution of both the polymer and a particular weight percent (e.g., 40 wt. % is designated by “-40-C”) of graphitized carbon particles (20 - 30 nm diameter; Polysciences, Inc.) in a solvent such as water or chlorobenzene. Typically, 0.1g of solids (polymer plus carbon particles) were dissolved in 5 mL of solvent. The polymers used were: poly(isobutylene) (PIB), ethyl cellulose (EC), poly(N-vinyl pyrrolidone) (PNVP), poly(diphenoxypyrophosphazine) (PDPP), poly(ethylene vinylacetate) (PEVA), and poly(vinyl alcohol) (PVA) that was 75% (PVA75), 88% (PVA88), and 98% (PVA98) hydroxylated. All polymers were purchased from either Polysciences, Inc. or Aldrich Chemical Company. The carbon loading typically ranged from 25 to 40 wt. %. The solutions, which contained agglomerated colloids of carbon, were treated with 15 half-second pulses using a point ultrasonic source with a one-second rest between pulses. In some cases a 5 μ m pore-size filter was used to enhance the dispersion of the carbon particles, which tended to agglomerate and form shorts between the narrowly spaced electrodes. The composite films were deposited on substrates by either spin casting or pipetting the dissolved material directly onto the substrate. Spin casting was performed at 3000 rpm for 30 seconds to yield approximately a 200 to 400-nm thick film². The pipette method usually led to films that were thicker and less uniform in thickness than the spin-cast films. All films were allowed to dry in ambient laboratory air by evaporation. Once dry, the two-point or, if applicable, the four-point resistance of each film was measured; some films had unacceptably high or low resistance values and were not used further.

The devices were placed in a specially designed test fixture, which had spring-loaded Pogo[®] pins (Newark electronics) to contact the pads on the substrates. The fixture was attached to a gas manifold that had the capability of mixing several gases as well as two solvent vapor streams, using nitrogen as the carrier gas through gas washing bottles (“bubblers”). The bubblers have a wide, porous ceramic frit at the base. Carrier gas (N₂, usually) is introduced into the solvent through a side arm and through the frit. The solvent-saturated gas mixture exits the

bubbler at the top and is then mixed with pure nitrogen to adjust the solvent concentration as desired. Table 1 contains the solubility parameters and vapor pressures of the eleven solvent vapors that were tested.

Mass flowmeters were used to control the composition of the gas streams, and a constant total flow rate of 1000 cm³/min was used for all experiments. The test fixture was placed in a constant-temperature chamber, which could be controlled to $\pm 0.1^{\circ}\text{C}$. A digital multimeter (7.5 digit resolution) was used to measure the composite-film resistance. The test gases were passed through a coil of tubing inside the constant-temperature chamber and upstream of the test fixture. This ensured that the inlet gas stream was thermally equilibrated with the sensors. The flow stream was then split into six parallel branches, with each branch directing flow over a different sensor in the test fixture. Data acquisition was performed using LabVIEW™ software on a personal computer to control the flow controllers and acquire data from the multimeters.

Results and Discussion

Pattern Recognition Data Analysis Techniques. The typical experiment consists of exposing the sensors to a known concentration of either a single solvent, or a binary mixture of two solvents, for 10 minutes. The DC resistance of the sensors was monitored continuously during the exposures and the relative change in resistance ($\Delta R/R_0$) from the baseline resistance was tabulated for each concentration set. Dividing all the data for one particular sensor by the largest response to any solvent exposure for that particular sensor is used to equalize the data for pattern-recognition purposes, such that the largest response is 1 for any particular sensor. The next mathematical operation is normalization, which creates unit vectors from, for example, the response of any three sensors (the x, y, and z coordinates). For the normalized data set (N_1, N_2, N_3), or unit vector, N_i is defined as:

$$N_i = \frac{E_i}{\sqrt{E_1^2 + E_2^2 + E_3^2}}, \quad (1)$$

where N_i is the new, normalized data point and E_i is the equalized data point corresponding to each of the three sensors ($i = 1,2,3$). Each different concentration set can be plotted on the surface of a unit sphere, with the relative response of each sensor as an orthogonal axis. This method can be used with any number of sensors (the surface is

a hypersphere if more than 3 sensors are involved). The sphere can be rotated to present, visually, the best separation of the responses for several solvents. Figure 1 shows that with three sensors based upon PVA75, PEVA, and PIB, pure solvents, such as DIMP, isoctane, ethanol, and water vapors can easily be distinguished as tight clusters of points. In this figure each point represents a different concentration of a single analyte (water or solvent vapor) or a binary mixture of the two vapors (water and solvent). The data from two independent experiments are presented in the figure, such that each combination of concentrations is repeated once. The responses to binary mixtures of each of the three organic solvents with water form solvent-specific “trails” of points, connecting the response cluster from pure water to that of the pure solvent.

The responses to an unknown mixture of two solvents could be plotted on a surface such as the sphere in Figure 1. The VERI (PR) method includes three general sorts of result for the classification of such a datum. If the new point were to fall on, or close to, one of the “trails” or clusters previously defined by the calibration data, it would be classified as either the corresponding pure solvent or a mixture of that solvent with water vapor. If the point were to fall in an area that is not close to any calibration data points, it would be classified as an unknown or “outlier” (rather than being misidentified, as might occur with some other PR methods). If the point were to fall close to two or more trails, the point would then have a certain probability of being classified as either of the two solvent mixtures: it would be classified as ambiguous. In all cases, the criteria for “close” to an established trail of points are defined by the VERI pattern-recognition algorithm¹⁹, which imitates the criteria that humans use to define a new point as clustering with an established group. For the case where the unknown point falls on a particular path—once the correct class or type of solvent has been identified—the two sensors exhibiting the greatest spread of responses from the two pure solvents are selected. For example, PVA75 and PEVA are the best choice to separate H_2O and DIMP, as shown in Figure 2. The relative responses ($\Delta R/R_0$) are presented in a two-dimensional “binary” plot, where the DIMP concentration is varied in the presence of a constant background of water vapor (i.e., relative humidity). The vapor-phase concentrations are presented as a percentage of the saturation vapor pressure (P_{sat}) or as a fraction, usually denoted P/P_{sat} , at the temperature of the vapor source. This type of plot can be used to linearly interpolate the concentrations corresponding to the unknown point, using the four known concentrations that surround it. To obtain the most accurate concentration estimate, however, any response non-linearities must be considered. Non-linearities in the observed absorption isotherm may be due to many factors, two of the principal

being extent of carbon loading and polymer type. The data from these sensors may be further analyzed by any pattern recognition method to classify the sensor responses; some of these methods will specify the “best” set of sensors, from among those tested, by determining the percentage of correct identifications. Pattern recognition techniques such as VERI or principal components analysis (PCA) can reduce the complexity and the dimensionality of the data set, making visual classification easier. PCA does this by seeking linear combinations of the responses from multiple sensors that maximize response differences, using each of these new combinations as an axis, so that high-dimensional responses can be reduced to two or three dimensions for visualization. VERI, on the other hand, selects the optimum subset of sensors from those tested; it is not invariably true that the optimum sensor set contains just two or three sensors³. An advantage shared by VERI and neural network analysis is that the concentration-dependent data need not be linear (nor be linearized) to be analyzed, in contrast to PCA.

Similar to other pattern recognition methods, the VERI algorithm uses the “leave-one-out” method to determine the number of correct classifications from the training data set of particular set of sensors. The entire data set, excluding one point, is classified, and then that point is replaced into the data set. This point is then determined by VERI to be correctly classified, incorrectly classified, an outlier, or part of multiple classes. Each data point is taken in turn and the statistics (percentage correct or incorrect) for the training set are tabulated. An optimized sensor array can be created by picking the set of sensors with the highest percentage of correct classifications for a given training set.³

Once a binary class for an unknown sample has been distinguished from other binaries or individual chemicals by an optimally large sensor array, then data from the training set for the two best sensors for that binary can be used to determine the individual concentrations in the binary sample, as shown in Figure 3. By using the best two sensors of those we examined, one can determine concentrations of binary mixtures of solvents and H₂O vapor. Using the same two sensors as in Figure 2, PEVA and PVA75, the ethanol/H₂O binary set can be determined, as well as the ethanol/methanol binary mixtures, although at low concentrations of methanol this is more difficult. This is remarkable considering that the solubility parameters of ethanol and methanol are so close (26.1 MPa^{1/2} and 29.7 MPa^{1/2}, respectively). Methanol/H₂O mixtures and isoctane/H₂O mixtures can be determined using PNVP and PEVA films.

The degree to which the data classes are separated from one another varies with the number of sensors used to perform the classifications. For the relatively simple case of 5 pure solvents, the optimum number of sensors is 3. Figure 4 shows 4 plots of the same data, using 2, 3, 4, and 5 different sensors, but projected into 2 dimensional space. All the data in Figure 4 have been radialized but not normalized. The process of radialization is a mathematical operation that doubles the distance of each data point from the origin, while keeping the same angle in space. This has the effect of separating the data near the origin, thereby enhancing the VERI algorithm's ability to classify responses from low concentrations of solvents by spreading similar data points. Using the VERI method, the data sets were rotated to present the best separation visually. Two sensors (PVA75-40-C and PDPP-40-C) can easily separate DIMP, isoctane and H_2O , but the ethanol and methanol data are still overlapping (Figure 4a). Other classification errors occur due to the shape of the classification template that is used¹⁹. For the 2-dimensional case, the horizontal bars indicate points that the VERI algorithm classified as outliers. The number of outliers can be reduced by acquiring more data to fill in the gaps between scattered data points.

The addition of PIB-40-C to the 2-dimensional sensor array results in a 100%-successful classification of all five solvents. As seen in Figure 4b, even ethanol, methanol, and H_2O are separated down to low concentrations ($P/P_{sat} = 1\%$). On each of the plots, the data points that are further from the center correspond to higher concentrations. The algorithm has no problem classifying the data correctly, although visually the ethanol, methanol, and isoctane data converge at the origin. Using PEVA-40-C as a 4th sensor in the array leads to another 100%-successful classification. Adding polymer films other than PEVA-40-C reduced the percentage of correct classifications by several percent. The PEVA film has the effect of further spreading all of the data radially from the origin. The addition of a 5th sensor to the set, specifically the PNVP-40-C sensor, actually reduces the overall percentage of correct identifications, due to the spreading of the H_2O data points. From Table 2, one can see that the percentage correct identifications actually decreases from 100% for 4 sensors to 97% when the 5-sensor array is considered in the calculations. This table contains the percentage correct identifications for the best possible sensor array for each number of sensors selected from a common set of 10 different sensors.

The statistics were tabulated from the results of a “leave-one-out” cross validation performed using the VERI algorithm. From Table 2, one can see that for the binary solvent mixture problem the percentage of correct identifications is maximized at 4 sensors, although that percentage is lower than that for the pure components. As

shown in Figure 5, a large portion of the binary mixture data, 76%, can be correctly identified using 4 sensors (PEVA, PVA, PIB, and PNVP). This figure contains two different views of the same data, which have been radialized, as an example of how some of the overlapping data can be viewed and distinguished by rotating the main data set. The pure isoctane, pure DIMP, DIMP + H₂O, and isoctane + H₂O classes are correctly identified by the algorithm, while the separation of ethanol, methanol and H₂O is much more difficult. In Figure 5, the larger circles are the points that were incorrectly identified (24%) either as multiple classes (21%), outliers (1.3%), or incorrect classes (2.2%). This suggests that even with the best 4-sensor array, those 4 sensors may not be adequate for certain applications, such as correctly distinguishing low concentrations of ethanol in water (70% correct) from methanol in water (40% correct). For example, when a small amount of methanol is added to a background of water vapor, these sensors may not be able to discriminate this event from the addition of more relative humidity. In comparison, when the VERI algorithm was applied to the data in Figure 1, 90% of the data were correctly classified, with only 4.6% classified as multiple classes and the rest classified incorrectly or as outliers. The difference between Figures 1 and 5 is that in Figure 1 no methanol data were included, so 3 sensors were almost adequate. Thus, the data in Figure 5 contain enough scatter or enough uncertainty at low concentrations for the VERI-PR program to misidentify quite a few individual data points.

Characteristics of Individual Chemiresistors. The problem of distinguishing the relative humidity in the background of unknown vapor mixtures requires a solution before sensors can be deployed in the field. Some devices can be quite sensitive to relative humidity: as shown in Figure 6, the PVA88 film responds to less than 0.25% relative humidity (~ 70 ppm absolute concentration of water vapor) in the nitrogen stream. The data from several different experiments on one particular PVA88 film are shown in this figure. The sensor shows better reproducibility in the range of 1 to 20% relative humidity. As the relative humidity increases, the film approaches its percolation threshold, and the response becomes less reproducible. When the relative humidity is less than 1%, the film shows some irreproducibility; however, this may be due to the lack of resolution in the mass-flow controllers. PVA has hydroxyl groups protruding from the polymer backbone, which endows this polymer with strong hydrogen bonding characteristics ($\delta \sim 25 - 30 \text{ MPa}^{1/2}$).²⁰ One can expect PVA to be highly sensitive to solvents with δ values in this range, as well as solvents that have the ability to hydrogen bond strongly.

The solubility parameter is a powerful measure of a polymer's tendency to absorb a particular solvent. Using δ , one can quickly determine which polymers will make good sensors for an array to span all of solvent space. The relative response of a particular film to many different solvents produces a map of solvent space on which the maximum response of a particular polymer can be located. Figure 7 contains the responses of several chemical sensors to 10% P/P_{sat} concentrations of individual solvents (Table 1) normalized to 1 using the largest response for each sensor. One can use such an analysis to determine which sensors are most sensitive to which range of solvents, and thereby create an array of varied films. Taking the same data for 3 sensors, one can normalize the responses and display the data on the surface of a unit sphere as in Figure 8. The responses to most of the 11 solvents can be separated using this method. From the plot, it is evident that several classes of chemicals may also be separated easily. For instance, water and the two types of alcohol, which are chemicals that have high δ values and strong hydrogen bonding characteristics, are separate from the other chemicals on the graph. On the other hand, it can also be seen that isooctane and cyclohexane are difficult to distinguish using these three sensors.

Discrepancies in the positions of data points on the graphs in Figures 1 and 8 arise from the normalization of the two independent data sets. Such plots can make choosing the correct sensors for a particular application easier. For example, these three sensors could be good candidates to separate ethanol, DIMP, isooctane, and water vapors, as was shown in the 3D plot in Figure 1. Since the PVA, PEVA, and PIB films are sensitive to solvents with different solubility parameters, they can be used to successfully distinguish the solvents. It is also apparent from Figure 7 that these films are not always selective to only one solvent, but respond to a variety of solvents with similar values of the solubility parameter.

Non-Superposition of Chemiresistor Responses to Binary Mixtures. On the binary plots (Figures 2 and 3) this lack of selectivity leads to nonlinearities and skewed responses. In other words, the response pattern is not a "perfect rectangle", as in the ideal case of each sensor responding to only one analyte. The resulting deviations from an ideal response are an attribute of the polymers' ability to absorb a significant amount of more than one solvent. For example, PVA75 responds strongly to water and methanol, and somewhat less to ethanol and other solvents with smaller δ values. This is translated into the methanol/ethanol binary plot as an increasing response (line with positive slope) with additional ethanol in the 20% methanol line.

Even with a particular sensing film responding to more than one analyte, one might expect the responses to be linear. However, some of the responses display curvature with increasing solvent concentration. As shown above in Figure 6, as the water concentration increases, the PVA88 film response deviates from linearity. Such responses are not simple linear combinations of the responses to the pure analytes; in other words, the responses are not superimposable, as shown in Figure 9. In this figure, the response of a PVA75 film is plotted against the relative humidity for cases where there was 0% methanol and 20% methanol in the background. The 0% methanol (i.e., H_2O in nitrogen only) case shows a relatively small response to 20% H_2O . When there is 20% methanol in the background stream, however, the sensor's response is large when the relative humidity is changed from 0 to 20%. In the third (simulated) data set, the value of each point of the 0%-methanol data is added to the single sensor response to 20% methanol and 0% H_2O . Clearly, this curve differs greatly from the real response, meaning that the responses of such sensors to individual analytes cannot be added to predict the responses to binary solvent mixtures. In this particular case, the nonlinear response is associated with the film approaching its percolation threshold at high solvent concentrations. This makes the accuracy and reproducibility of the binary calibration data sets very important to determining the actual concentrations of both solvents. Nonlinear sensor responses may render some chemometric algorithms impotent, requiring the use of VVERI or neural networks to analyze these systems correctly.

The nonlinearities are associated with two parameters in the present work: the chemical identity of the polymer and the extent carbon loading. Nonlinearities in the response to a single solvent, such as water vapor in Figure 6, can usually be attributed to the degree of carbon loading: when the film is near the percolation threshold, the next small addition of analyte causes a disproportionately large increase in resistance.

For samples with different amounts of carbon in a particular polymer, the overall resistance increases as the percentage carbon loading is decreased. For instance, chemiresistors made from PEVA films with 15 to 20% carbon loading were found to have resistances in excess of 1 $\text{G}\Omega$ in laboratory air for the 6 mm long Pt electrodes separated by 50 μm , while samples with greater than 25% carbon loading were typically in the range of 10 $\text{k}\Omega$ to 5 $\text{M}\Omega$, depending on deposition method, filtration, and precise carbon concentration. The effects of swelling due to thermal expansion upon carbon/polymer composite resistance properties have been studied in detail.^{12,13} The resistance is found to increase superlinearly with thickness when such composite films are heated, an effect that is

probably associated with thickness-dependent variability in the rate at which existing percolation paths are lost as the film is made thicker.

In the case of the present films, as the carbon loading decreases in a particular film, the sensor response becomes less linear with solvent concentration. This is due to the fact that the film, at lower carbon loading, is closer to the percolation threshold and small increases in solvent concentration lead to proportionately larger resistance increases.

Contact Resistance Effects in Measuring Film Resistance. In some cases, especially when there is a great deal of swelling in the film, the contact resistance between the sensing film and the electrodes was found to increase with increasing solvent concentration, as shown in Figure 10. In cases of extreme swelling, a total loss of contact was observed. Using four-terminal resistance measurements can eliminate the large and varying contact resistance values. As shown in Figure 10, the two-terminal and four-terminal resistance responses are similar at low TCE concentrations; however, above 10% the two values are quite different, a consequence of the contact resistance, which increases as the polymer swells. For this particular sensor, the contact resistance is on the order of the bulk, 4-terminal resistance. The contact resistance makes the response appear to be more sensitive than it really is, but, in actuality, the sensor response is less reproducible, because the contact resistance changes over time, and with different exposures. Also, the contact resistance varies greatly from device to device depending on many factors, such as film composition, carbon loading, deposition method, and polymer adhesion.

Cononsolvency Effects in Chemiresistor Response to Binary Mixtures. In some binary solvent experiments, where the solubility parameters of the two solvents, or the polymer and one of the solvents, vary greatly, the addition of the second solvent to the system can diminish the solubility of the first solvent leading to a decrease in film resistance. This exclusion or rejection of a solvent has been observed in particular solvent/polymer combinations, and is called cononsolvency²¹. Figure 11 shows the relative response of the PEVA-40-C sensor to water vapor and isoctane/water mixtures. This behavior is observed in experiments where the isoctane is present first, with H₂O added in steps, as in Figure 11, and also in experiments where the H₂O is present first, and the isoctane is added in steps. Such phenomena have been attributed to a change in the film polarity as the polymer absorbs significant amounts of a particular solvent⁶. In the case of PEVA ($\delta \sim 16 - 22 \text{ MPa}^{1/2}$)²⁰, it seems that the high concentration of isoctane makes the film less polar, and the addition of a high concentration of H₂O forces

some of the isoctane back out of the film. For instance, when the PEVA film is exposed to isoctane at concentrations greater than $P/P_{sat} = 5\%$, and then H_2O vapor is added, the sensor resistance decreases by up to 4% of the full-scale response (0% H_2O & 20% isoctane) for 40% relative humidity and 20% isoctane. The total resistance decrease corresponds to approximately a 3% decrease in the isoctane concentration if no H_2O were present. The resistance decrease is related to a positive deviation from Raoult's law. When two immiscible liquids, such as water and isoctane, are mixed, a positive deviation from Raoult's law results because the interaction between the two types of solvent molecules is unfavorable and the solution has an excess Gibbs energy that is greater than zero. In contrast, with concentrations of 5% isoctane or less, the resistance increases by only 0.4% from baseline (0% H_2O & 5% isoctane) when 40% relative humidity is added. This response is expected, since it is similar to the response of the PEVA film to the same H_2O exposure with no isoctane present.

In some cases, the polymer film may take the place of the second solvent, resulting in an immiscible solvent-polymer mixture. Such a response has been observed with PIB films during the addition of water vapor. PIB is a very nonpolar film, as reflected by its Hansen parameters²⁰, which are 15.7 and 0.0 MPa^{1/2}, for the nonpolar and polar parameters, respectively. The overall solubility parameter for PIB²⁰ is approximately 15 - 16 MPa^{1/2}, so the PIB film can be expected to absorb very little, if any, H_2O .

Yet a third sort of response is displayed by films typified by the relatively polar material polyvinyl alcohol, which shows a similar (cononsolvency) decreasing resistance response when isoctane is added in the presence of high concentrations of water vapor. The polyvinyl alcohol films have a much higher solubility parameter and stronger hydrogen bonding character than isoctane. The PVA films behave in the opposite manner, compared to PEVA, with the large H_2O concentration making the film more polar, and the addition of a small amount of isoctane forcing some of the H_2O out. As shown by Figure 7, the relative response of PEVA to isoctane can be an order of magnitude greater than to H_2O , while the opposite is true for PVA films.

Summary and Conclusions

Carbon-loaded polymer films make effective, low-cost sensors for solvents and binary mixtures of solvent vapor and relative humidity. The carbon particles act as conductive pathways, some of which break when the film swells during solvent absorption. Two important conclusions from our work are: (1) contact resistance can

adversely affect accuracy and reproducibility, suggesting the use of 4-point measurements for applications that include the analysis of relatively high solvent concentrations, and (2) increasing the size of an array does not invariably increase accuracy of identification, and can actually have the opposite effect, as shown in Table 2.

By selecting the appropriate set of three sensors, normalizing and equalizing the data appropriately, and then plotting the resulting 3-D data in a 2-D projection of a unit sphere, it is possible to classify visually the responses to several analytes: DIMP, ethanol, isoctane, and H₂O vapors. New data points can be identified correctly according to their proximity relative to the clusters of points created by the calibration data. The polymers upon which this sensor array is based were chosen to respond to solvents over a wide range of solubility parameters.

Using the same set of three sensors, binary mixtures of water vapor and solvent vapor can be classified with better than 90% accuracy. However, only 76% accuracy is achieved using 4 sensors when data from exposures to pure methanol and methanol/water mixtures are added to the original data set. The responses to binary mixtures form "trails" on the unity sphere's surface, which aid in quantification of concentrations. Once the solvent mixture is classified by composition, binary calibration data sets are used to quantify solvent and H₂O concentrations. Accuracy is reduced when these "trails" overlap due to similarity in the response to more than one analyte. Polyethylene vinylacetate and polyvinyl alcohol are two polymers that have been used to quantify binary mixtures of DIMP with water vapor; the PVA88 films respond to less than 0.25% relative humidity. The sensor responses were found to be non-linear at high solvent concentrations and also non-additive with some binary mixtures. These nonlinear responses generally restrict the type of chemometrics algorithms that can be used effectively in analyzing sensor array data, but they do not adversely affect results from the Sandia VERI method.

Acknowledgements

The authors would like to thank Rubel Martinez for his assistance with the VERI algorithm. Sandia is a multiprogram laboratory operated by Sandia Corporation, a Lockheed Martin Company, for the United States Department of Energy under Contract DE-AC04-94AL85000.

References

- [1] Freund, M. S.; Lewis, N. S. *Proc. Natl. Acad. Sci. USA* **1995**, 92, 2652.
- [2] Lonergan, M. C.; Severin, E. J.; Doleman, B. J.; Beaber, S. A.; Grubbs, R. H.; Lewis, N. S. *Chem. Mater.* **1996**, 8, 2298.
- [3] Osbourn, G. C.; Bartholemew, J. W.; Ricco A. J.; Frye, G. C. *Acc. Chem. Res.* **1998**, 31, 297.
- [4] Nagle, H. T.; Schiffman, S. S.; Gutierrez-Osuna, R. *IEEE Spectrum*, **1998**, 35, 22.
- [5] Domanský, K.; Baldwin, D. L.; Grate, J. W.; Hall, T. B.; Li, J.; Josowicz, M.; Janata, J. *Anal. Chem.* **1998**, 70, 473.
- [6] Zellers, E. T.; Han, M. *Anal. Chem.* **1996**, 68, 2409.
- [7] Ballantine, D. S.; Rose, S. L.; Grate, J. W.; Wohltjen, H. *Anal. Chem.* **1986**, 58, 3058.
- [8] McGill, R. A.; Abraham, M. H.; Grate, J. W. *CHEMTECH* **1994**, 24, 27.
- [9] Eastman, M. P.; Hughes, R. C.; Yelton, W. G.; Ricco, A. J.; Patel, S. V.; Jenkins, M. W. "Application of the Solubility Parameter Concept to the Design of Chemiresistor Arrays," submitted to *Journal of the Electrochemical Society*.
- [10] Hughes, R. C.; Eastman, M. P.; Yelton, W. G.; Ricco, A. J.; Patel, S. V.; Jenkins, M. W. *Tech. Digest of the 1998 Solid-State Sensor and Actuator Workshop*, Transducers Research Foundation: Cleveland, 1998, pp. 379-382.
- [11] Hampl, J.; Bouda, V. *Synthetic Metals*, **1994**, 67, 129.
- [12] Heaney, M. B. *Appl. Phys. Lett.* **1996**, 69, 2602.
- [13] Heaney, M. B. *Physica A*, **1997**, 241, 296.
- [14] Viswanathan, R.; Heaney, M. B. *Phys. Rev. Lett.* **1995**, 75, 4433.
- [15] Grate, J. W.; Kaganove, S. N.; Bhethanabotla, V. R. *Anal. Chem.* **1998**, 70, 199.
- [16] Barton, A. F. M. *CRC Handbook of Solubility Parameters and Other Cohesion Parameters*, CRC Press, Inc.: Boca Raton, Florida, 1983; Chapter 7.
- [17] Riddick, J. A.; Bunger, W. B.; Sakano, T. K. *Organic Solvents, Physical Properties and Methods of Purification*, 4th ed.; John Wiley & Sons: New York, 1986; Chapter 3.
- [18] Kepley, L. J.; Crooks, R. M.; Ricco, A. J. *Anal. Chem.* **1992**, 64, 3191.

- [19] A description of the VERI algorithm and the human vision research that is the basis of the algorithm can be found at <http://www.sandia.gov/1100/1155Web/users.htm>.
- [20] Barton, A. F. M. *CRC Handbook of Solubility Parameters and Other Cohesion Parameters*, CRC Press, Inc.: Boca Raton, Florida, 1983; Chapter 13.
- [21] Barton, A. F. M. *CRC Handbook of Solubility Parameters and Other Cohesion Parameters*, CRC Press, Inc.: Boca Raton, Florida, 1983; p. 245.

Tables

Table 1: Solubility Parameters and Vapor Pressures of Solvent Vapors

Chemical	Solubility Parameter ^{ref} (MPa ^{1/2})	Vapor Pressure ^{ref} (Torr) at 23°C
Isooctane	14 ¹⁶	45 ¹⁷
Cyclohexane	16.8 ¹⁶	89 ¹⁷
m-Xylene	18.2 ¹⁶	7 ¹⁷
Toluene	18.3 ¹⁶	26 ¹⁷
Trichloroethylene	18.7 ¹⁶ (20.2 ⁹)	68 ¹⁷
Acetone	19.7 ¹⁶ (20.5 ¹⁷)	212 ¹⁷
DIMP	20 ⁹	0.7 ¹⁸
DMMP	21.8 ⁹	2-5 ⁹
Ethanol	26.1 ¹⁶	52 ¹⁷
Methanol	29.7 ¹⁶	114 ¹⁷
Water	48 ¹⁶	21 ¹⁷

Table 2: Results of the “Leave-One-Out” Analysis for Pure Solvents and Binary Mixtures

Sensors	% Correct Classifications (5 Pure Solvents)	% Correct Classifications (Binary Mixtures with H ₂ O)
2	91	54
3	100	64
4	100	76
5	97	75
6	96	75
7	94	72
8	94	68
9	91	65
10	77	60

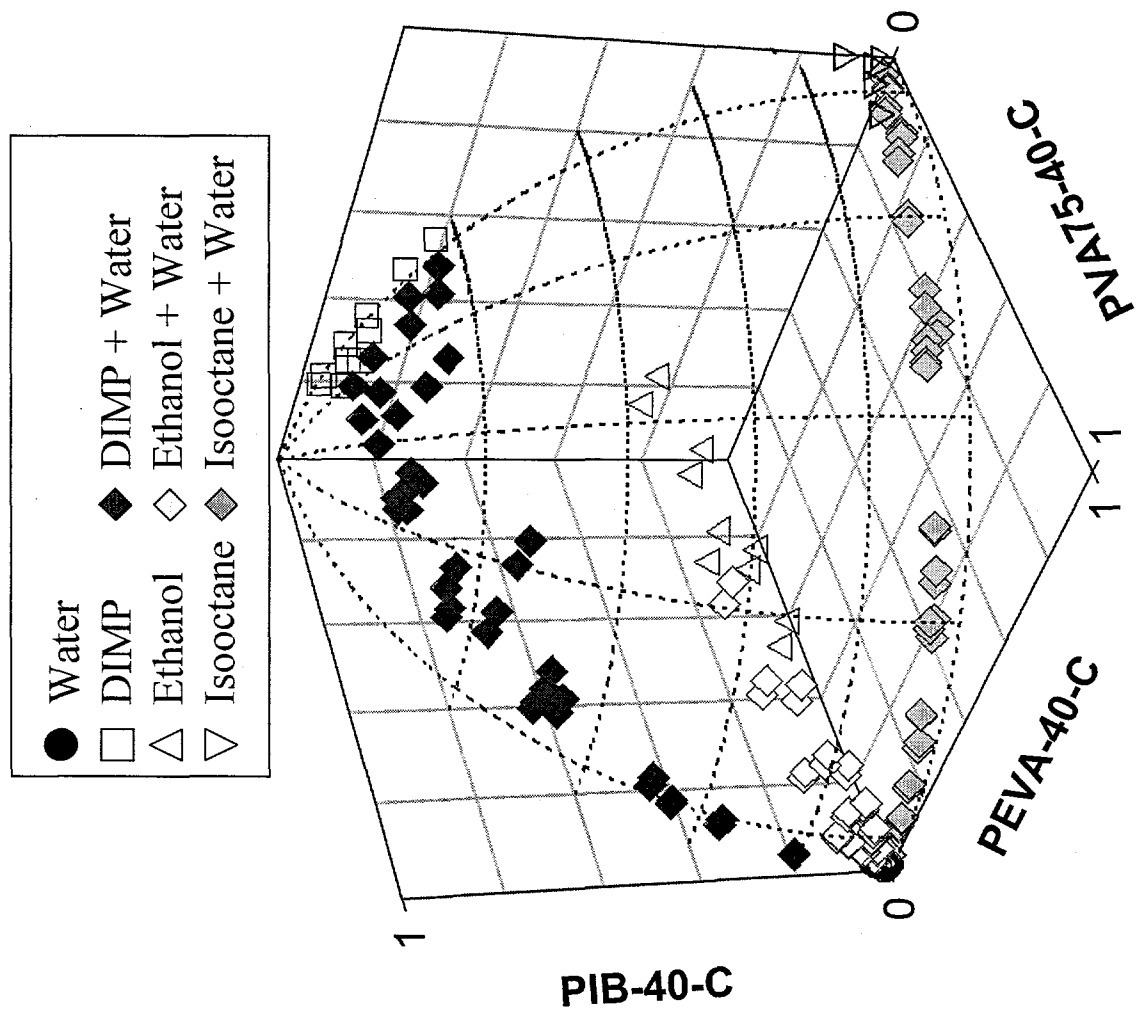
Figure Captions

- 1) The normalized responses of three sensors (PVA75-40-C, PEVA-40-C, and PIB-40-C) at 23°C to DIMP, ethanol, or isoctane, mixed with water vapor, are plotted on the surface of a unit sphere. The three axes are the normalized responses of each sensor. The sphere can be rotated until each solvent is visually distinguishable. The responses to binary mixtures of solvent and water vapor form “trails” on the surface of the sphere from pure water vapor to the pure solvent.
- 2) The relative response ($\Delta R/R_0$) of two chemiresistor sensors, at 23°C, to combinations of DIMP and water vapors are plotted. Vapor-phase concentrations (P/P_{sat}) are presented as percentages of the saturated vapor pressures. $P/P_{sat} = 100\%$ corresponds to approximately 920 ppm absolute concentration of DIMP. In this set of experiments, each line represents a different background relative humidity and each point represents a different DIMP concentration.
- 3) Different sensors are used to provide separation of concentrations for binary mixtures of solvents. The sensors and solvents were maintained at 22 - 23°C during the experiments, and the solvent concentrations (P/P_{sat}) were: (a) ethanol = {0, 1, 3, 5, 10, 20%} & water = {0, 5, 10, 20, 40%}; (b) methanol = {0, 1, 3, 5, 10, 20%} & water = {0, 5, 10, 20, 40%}; (c), methanol = {0, 1, 3, 5, 10, 20%} & ethanol = {0, 5, 10, 20, 40%}; (d) isoctane = {0, 1, 3, 5, 10, 20%} & water = {0, 5, 10, 20, 40%}. Each line represents a constant concentration of one species, and each point represents a different concentration of the other species.
- 4) The graphical results (2-dimensional projections) showing the separation of the radialized responses to 5 pure solvents by sensor arrays containing 2, 3, 4, and 5 different sensors. The percentage correct classifications is 100% for the 3- and 4-sensor cases. The responses to higher concentrations of solvents appear further from the origin on each plot. With more than 4 sensors in the array, the data are more spread out, causing more errors in classification.
- 5) The 2-dimensional graphical representation of a 4-sensor array response to water, ethanol, methanol, DIMP, isoctane, and each of the latter 4 organic solvents mixed with water. The figure contains two views of the same data to show how rotation can aid the separation of classes. View (a) shows the separation of pure DIMP, pure isoctane and the binary mixtures of water with each of these. View (b) shows the separation of pure ethanol and water, while the ethanol + water, and methanol + water binary data remain overlapped.
- 6) The PVA88-40-C sensor response at 23°C is plotted versus relative humidity. The inset shows that the response is linear at low concentrations, but the response deviates from linearity at higher H_2O concentrations as the polymer swells. The data were collected using a 4-terminal resistance measurement to eliminate any nonlinearities due to contact resistance effects.
- 7) The relative responses of several sensors are plotted versus solubility parameter. The solvents' solubility parameter values (Table 1) range from 14 to 48 MPa^{1/2}. Peak response corresponds approximately to the solubility parameter of the polymer film. The sensors were exposed to 10% of the saturation vapor pressure of each solvent, with the sensors and solvents at 23°C.
- 8) The normalized responses of the three sensors (PVA75-40-C, PEVA-40-C, and PIB-40-C) from Figure 1 to 11 solvents is presented on the surface of a unit sphere. The response is to $P/P_{sat} = 10\%$ for each solvent individually, with the sensors and solvents at 23°C.
- 9) The response curves of a PVA75-30-C sensor to various methanol and water vapor mixtures, at 23°C, shows that the sensor responses are not simple linear combinations of the responses to the individual components. This makes binary calibration data sets (Figures 2 and 3) important to the accurate determination of the solvent and water vapor concentrations. The data were collected using a 4-terminal

resistance measurement. Nonlinearities are affected by carbon particle concentration in the film and the chemical composition of the polymer.

- 10) The response of a PEVA-40-C sensor to trichloroethylene from $P_{sat} = 1 - 40\%$. The resistance changes from baseline (ΔR) for both two- and four-terminal measurements, as well as the contact resistance values, are plotted. The contact resistance increases with increasing solvent concentration, i.e., when the polymer swelling is large.
- 11) The response of a PEVA-40-C sensor to water and isooctane mixtures. As the isooctane concentration is increased in the background, the response to relative humidity decreases. Each line represents a constant isooctane concentration, and each point represents a different water concentration ($P_{sat} = 0, 5, 10, 20, 40\%$).

Figure 1



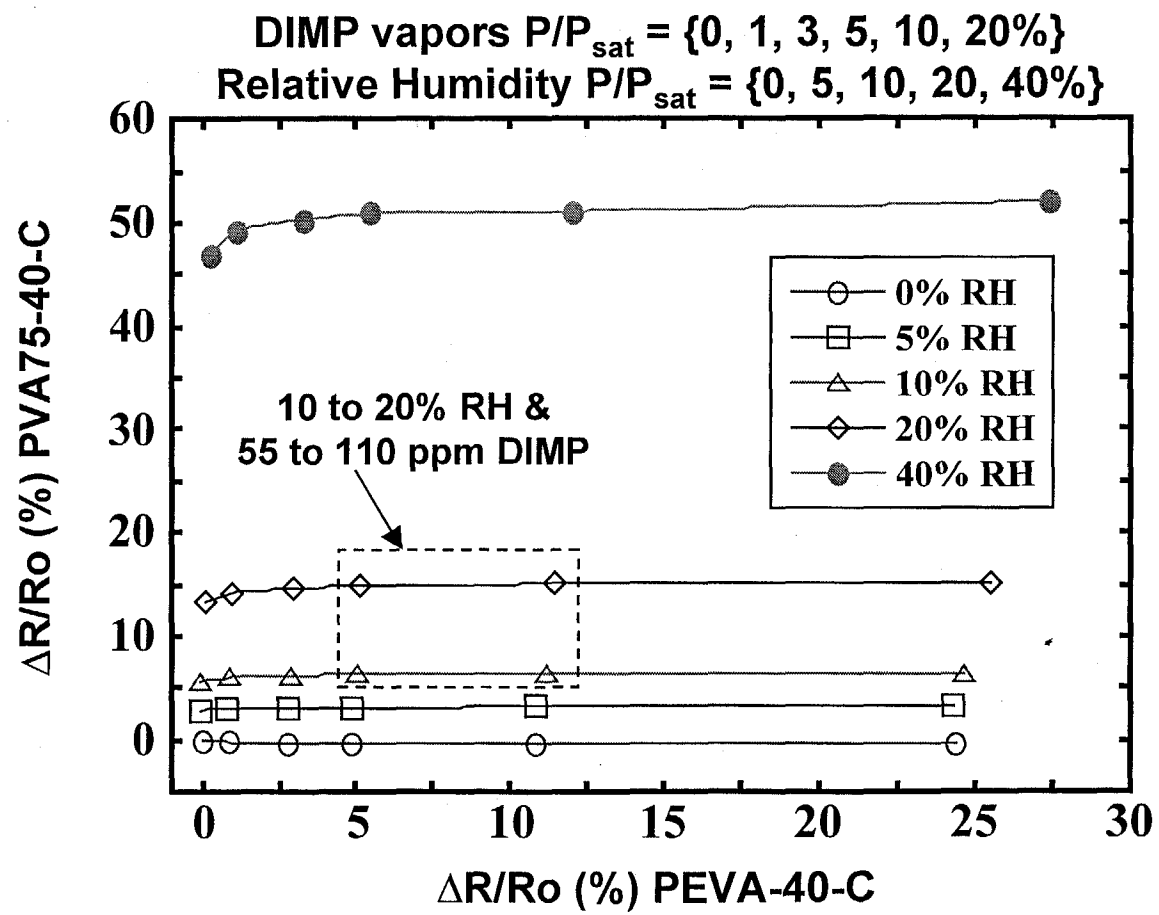


Figure 2

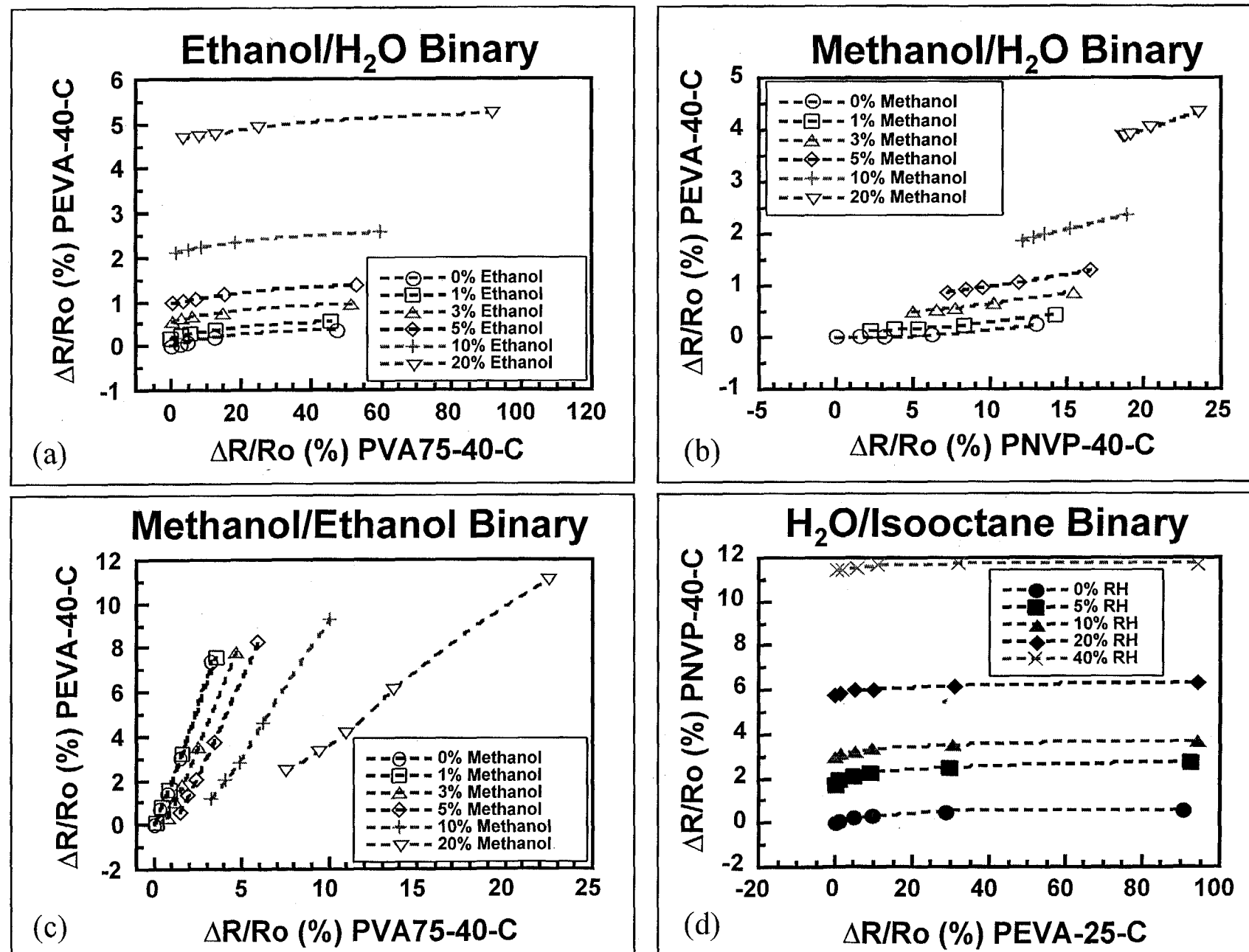


Figure 3

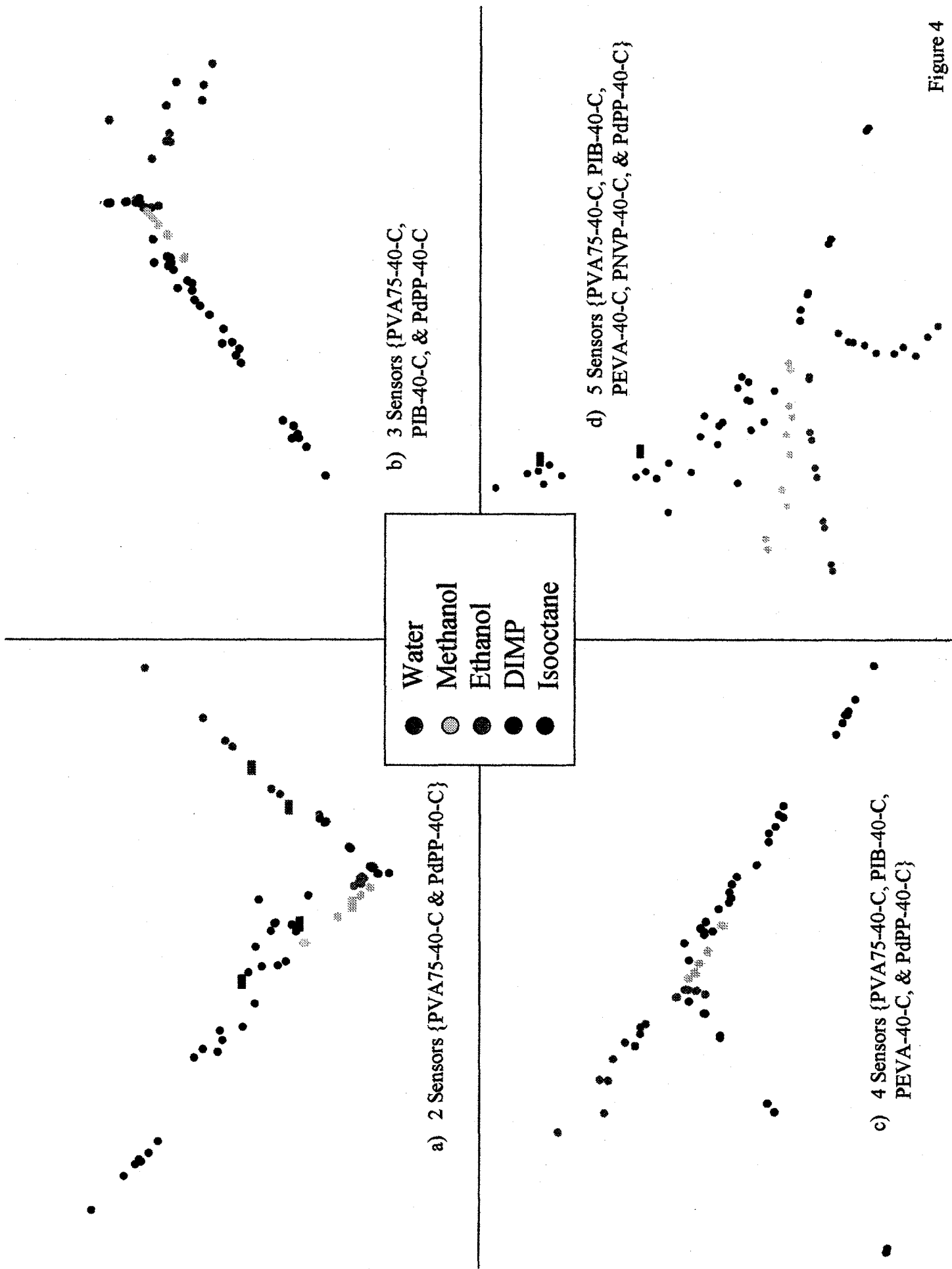


Figure 4

Figure 5

(a) (b)

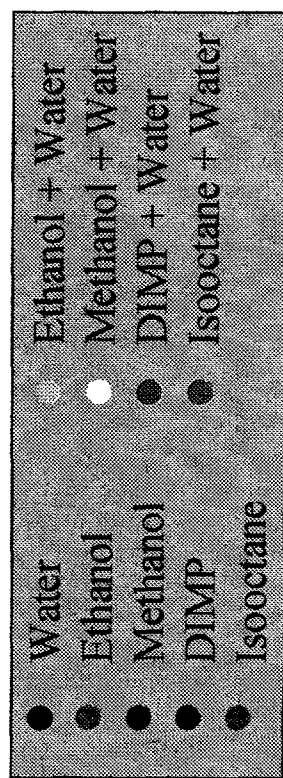
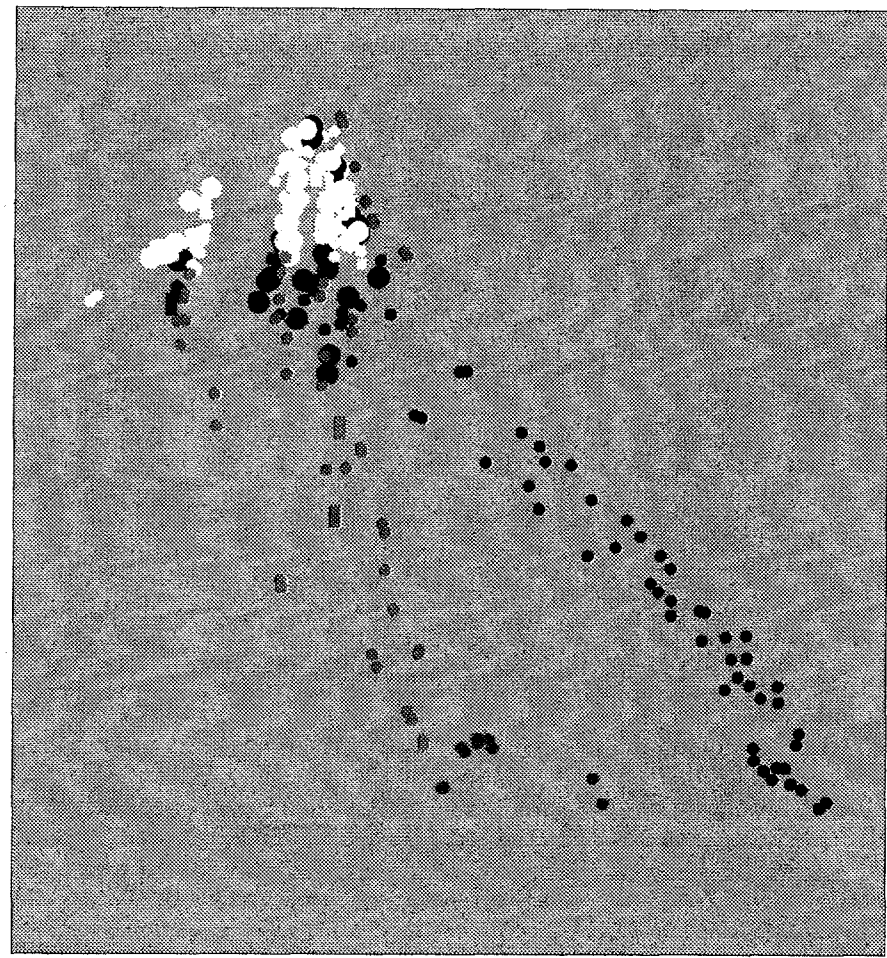
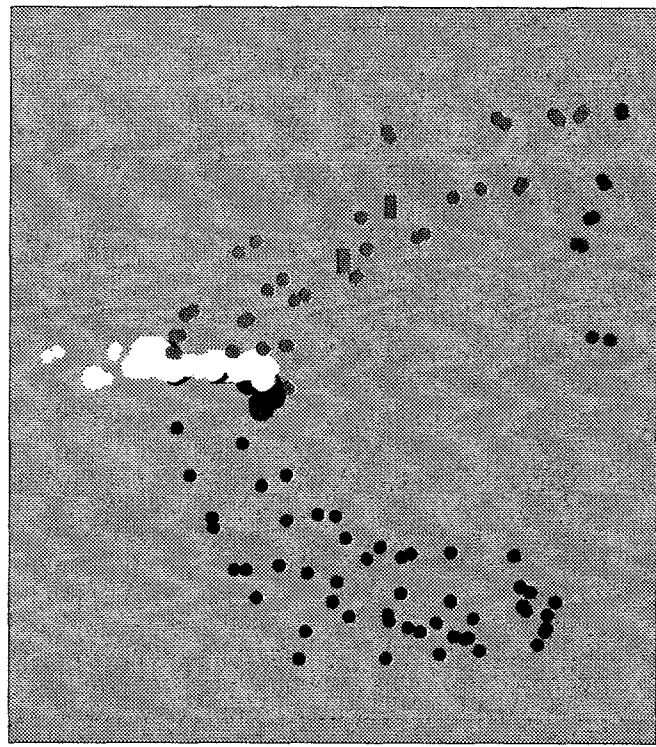
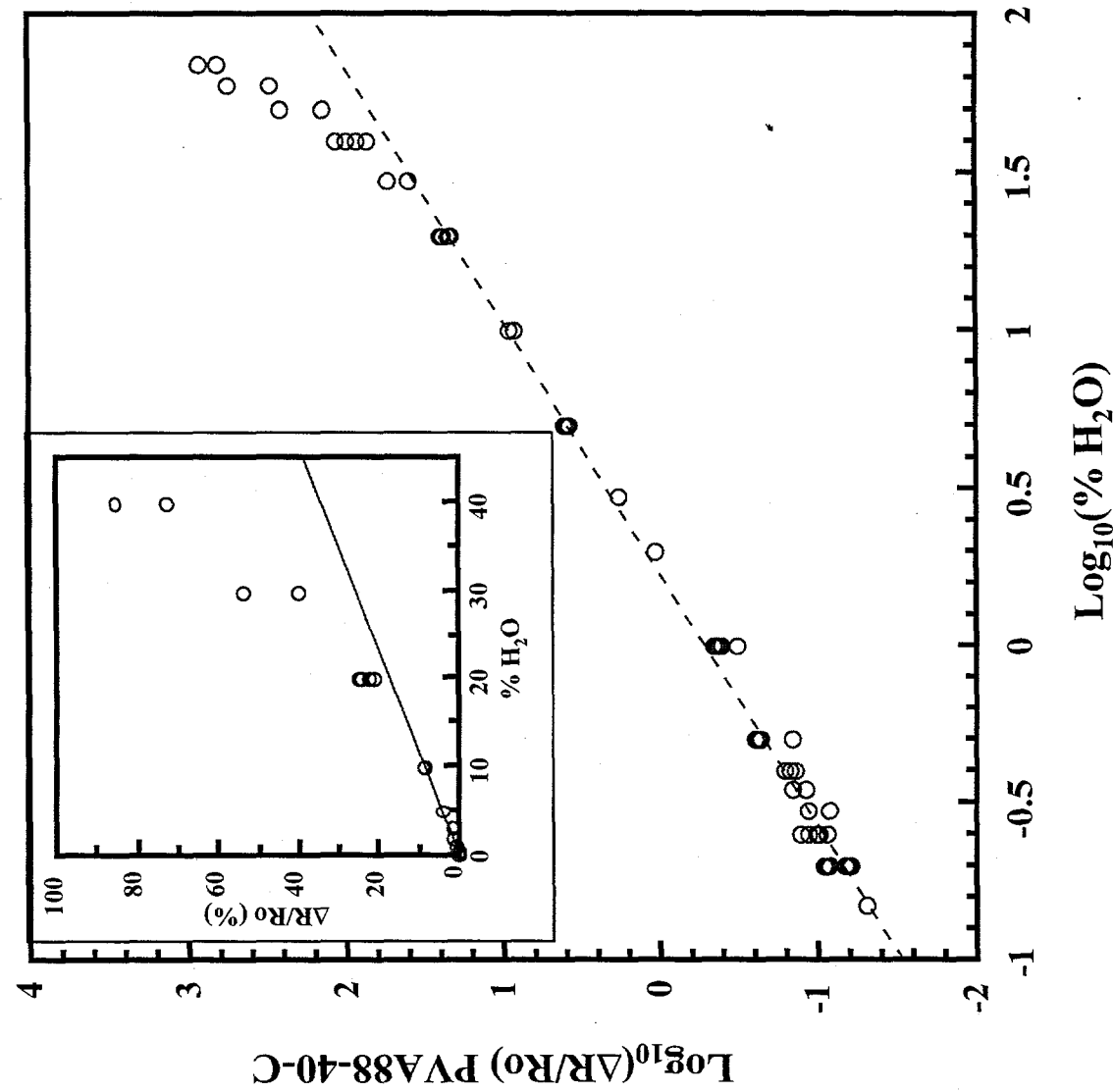


Figure 6



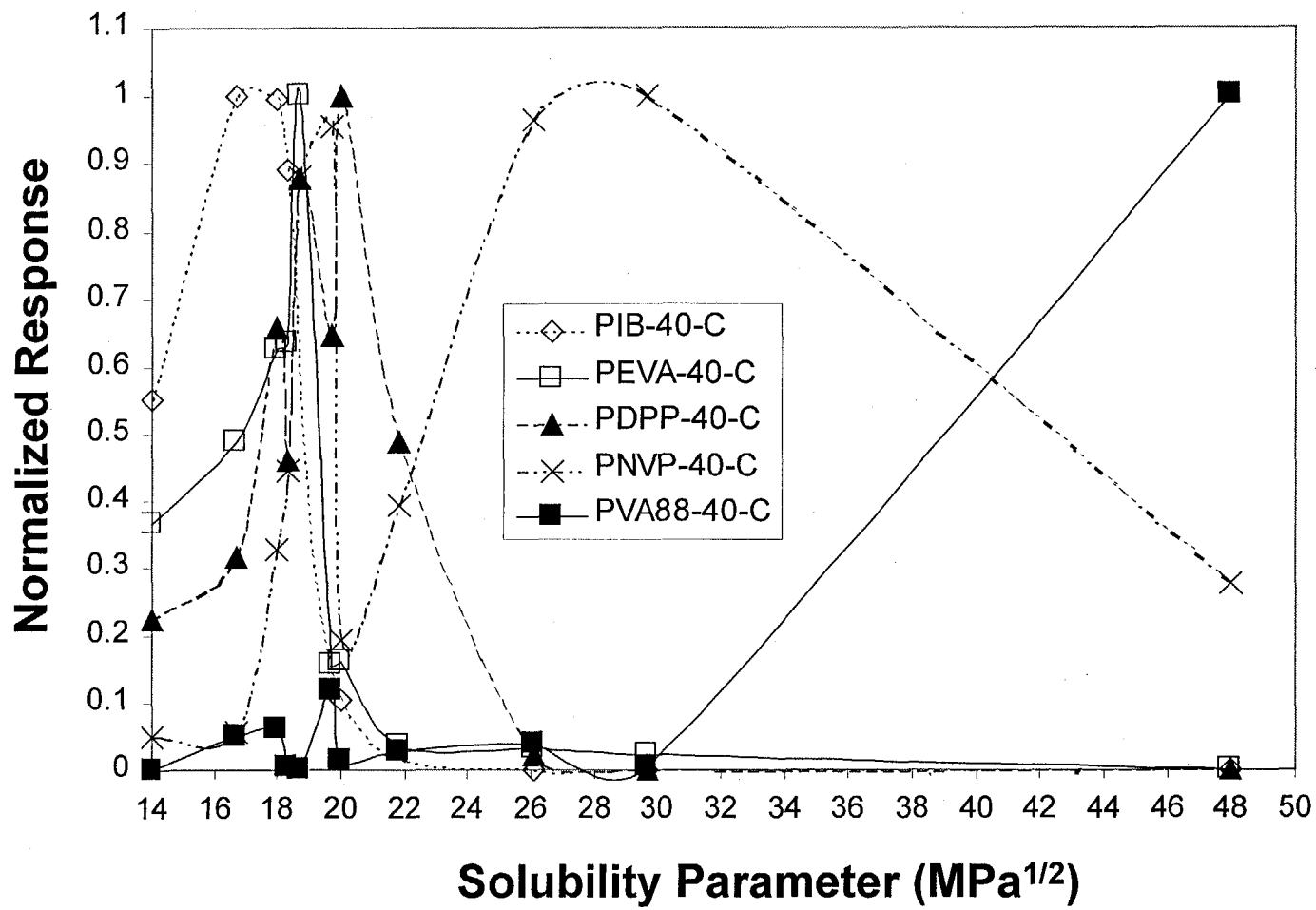


Figure 7

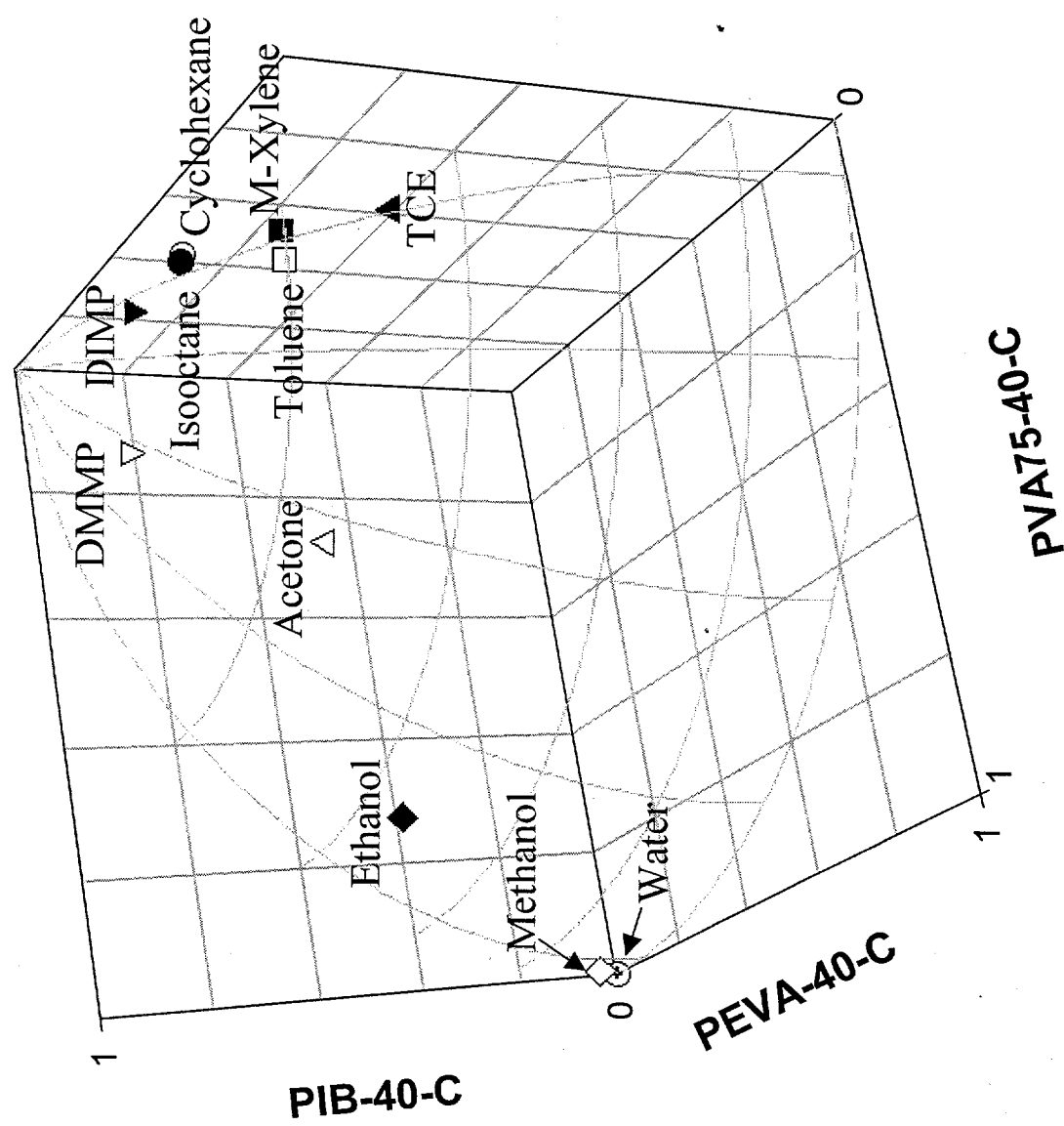


Figure 8

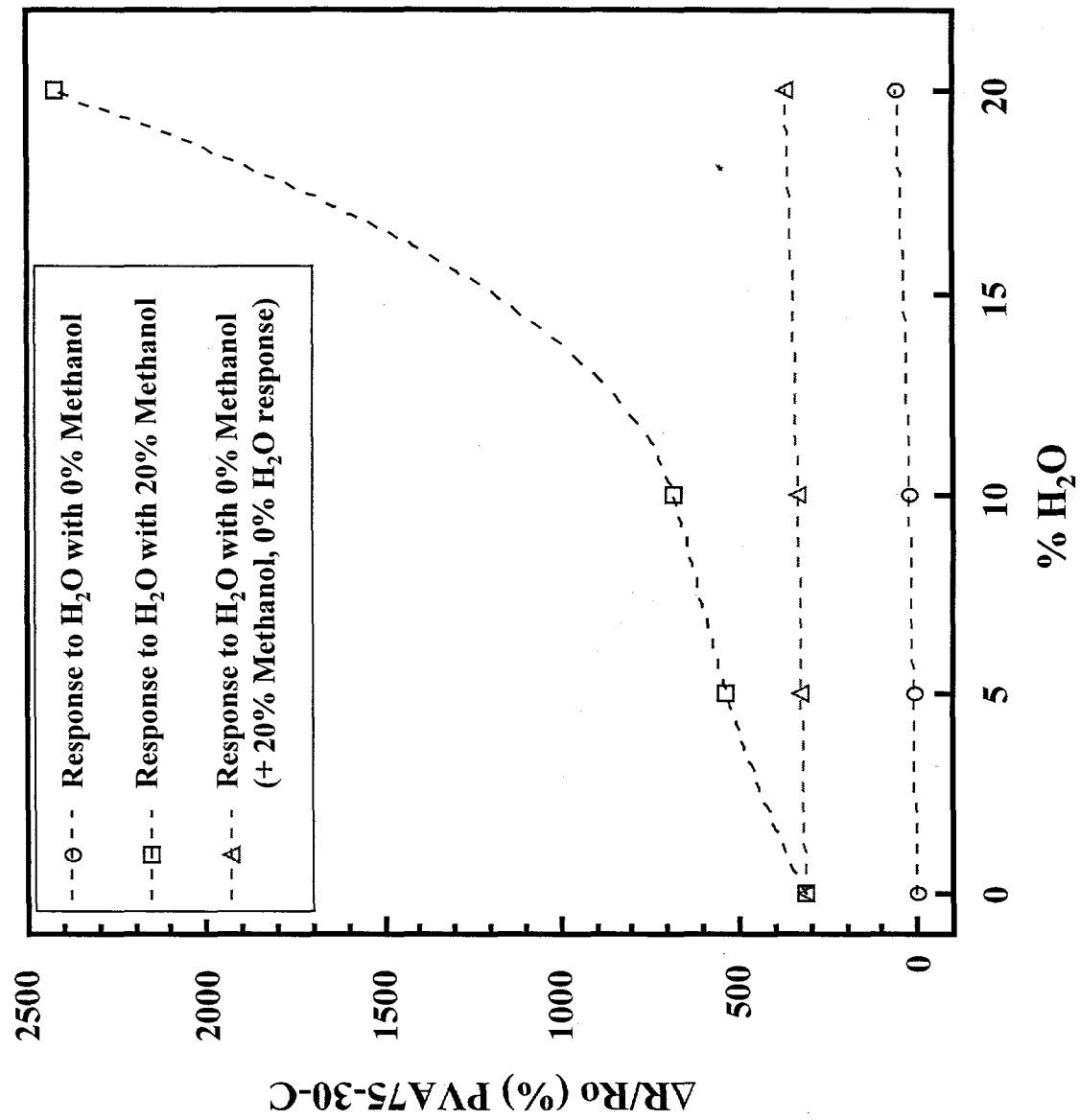


Figure 9

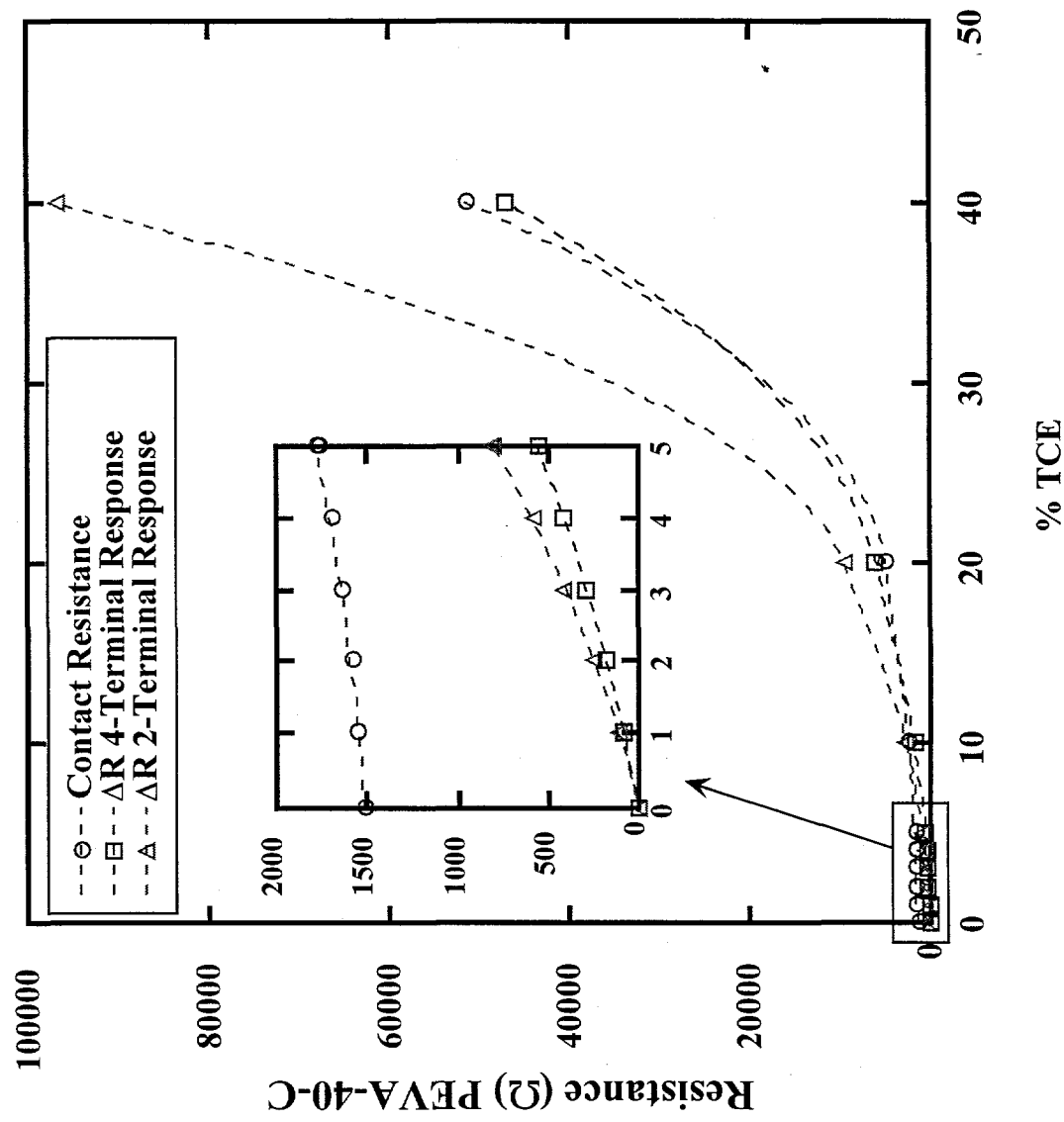


Figure 10

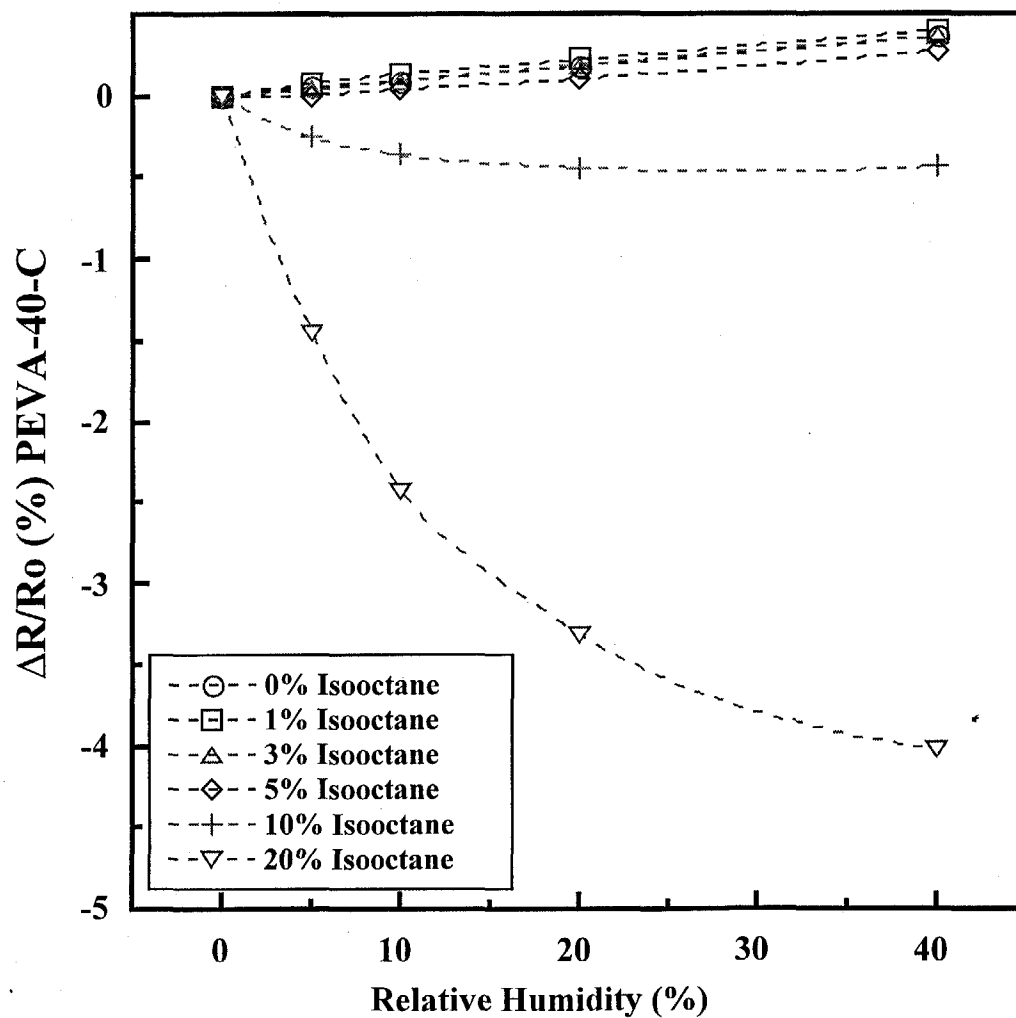


Figure 11